Eur. Phys. J. D **37**, 177–180 (2006)
DOI: 10.1140/epjd/e2005-00311-6

THE EUROPEAN PHYSICAL JOURNAL D

Average fluorescence yields of $M_{4,5}$ subshells for thorium and uranium

E. Tıraşoğlu[a]

Department of Physics, Faculty of Arts and Sciences, Karadeniz Technical University, 61080 Trabzon, Turkey

Received 23 July 2005 / Received in final form 15 September 2005
Published online 16 November 2005 –

Abstract. $M_{4,5}$ subshells average fluorescence yields ($\varpi_{M_{4,5}}$) have been determined for thorium and uranium using $M_{4,5}$ X-ray production cross-sections at 5.96 keV incident photon energy. The measurements have been performed using a ^{55}Fe annular source and an Ultra-LEGe detector. The present values are compared with calculated theoretical values and theoretical average M shell fluorescence yields (ϖ_M). Fair agreement (to within 22–27%) is typically obtained between present average fluorescence yields ($\varpi_{M_{4,5}}$) and calculated theoretical values.

PACS. 32.30.Rj X-ray spectra – 32.80.Cy Atomic scattering, cross sections, and form factors; Compton scattering

1 Introduction

K and L shell X-ray production cross-section data have been studied extensively whereas measured M shell X-ray production cross-section data are scarce, due in part to the complexity associated with the M shell X-ray spectrum. The number of transitions from higher shells which can fill an M shell vacancy is much greater than for K or even L shell vacancies.

Through the literature we have found no experimental values reported for the $M_{4,5}$ X-ray production cross-sections of Th and U. Gowda et al. [1] have reported M shell X-ray production cross-sections in Ir, Pt, and Pb due to the bombardment of $^4He^+$ ions of energy 0.4–2.2 MeV. Pajek et al. [2] have measured M shell X-ray production cross-sections for ten elements for protons of energy 0.6–4 MeV. Braich et al. [3] have measured the M shell X-ray cross-section in Pb due to the impact of protons and nickel ions. Amirabadi et al. [4] have measured M shell cross-sections of Hg at 0.7–2.9 Mev. Sing et al. [5,6] have reported M shell X-ray production cross-sections for Au and Bi induced by F ions in the energy range of 20 to 102 MeV. Shatendra et al. [7] have measured M shell fluorescence cross-sections for Au, Pb, Th and U, using a ^{55}Fe radioactive source. Garg et al. [8] measured M shell X-ray production/fluorescence (M XRF) cross-sections for five elements in the range $81 \leq Z \leq 92$ at 5.96 keV.

M shell fluorescence yields of Bi, Pb, Au and Os have been determined by Jopson et al. [9]. Deutsch et al. [10] have reported the $L_{2,3}$ and $M_{2,3}$ fluorescence yields of Cu. Rao et al. [11] have measured average M shell fluorescence yields for Pt, Au and Pb at $5.47 < E < 9.36$ keV. Apaydin et al. [12] have measured total M shell X-ray production cross-sections and average fluorescence yields for some heavy elements at photon energy of 5.96 keV.

In the present work, $M_{4,5}$ X-ray production cross-sections for Th and U have measured by 5.96 keV photons. Average shell fluorescence yields for $M_{4,5}$ subshells have been evaluated from present experimental $M_{4,5}$ X-ray production cross-sections and photoionization cross-sections.

2 Experimental details

Measurements of cross-sections for the production of M_i sub-shell X-rays of Th and U were made. The studied compounds were $ThOCO_3 \cdot H_2O$ and $UO_2(CH_3COO)_2 \cdot 2H_2O$. The purity of commercially obtained materials was better than 99%. Powder samples were sieved to 400 mesh sizes and prepared by supporting the powder on scotch tape $\cong$ 10 mg/cm^2 thickness. The experimental geometry is shown in Figure 1. The samples were irradiated by 5.96 keV photons emitted by an annular 1.85 GBq ^{55}Fe radioactive source. The incident beam and fluorescence X-rays emitted from the target were detected and analyzed with a Ultra-LEGe detector (FWHM 150 eV at 5.9 keV, active area 30 mm^2, thickness 5 mm and polymer window thickness 0.4 μm). The output from the preamplifier, with pulse pile-up rejection capability, was fed to a multi-channel analyzer interfaced with a personal computer provided with suitable software for data acquisition

[a] e-mail: engint@ktu.edu.tr

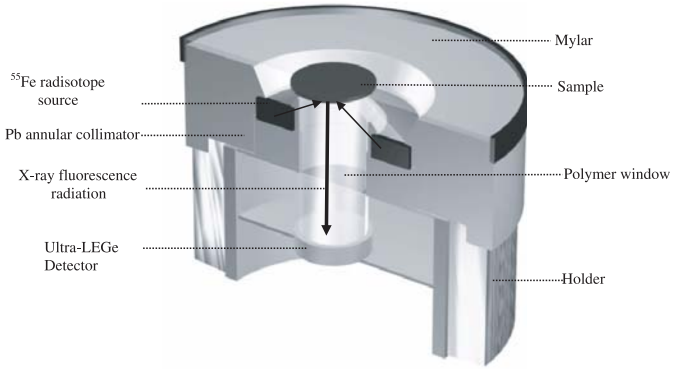

Fig. 1. Geometry of experimental set-up.

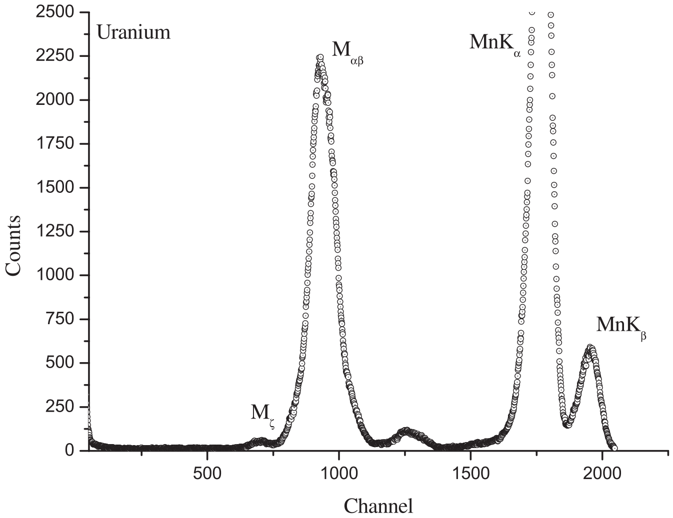

Fig. 2. M shell X-ray spectrum of U in collision with 5.96 keV photons.

and a fit program were used for peak analysis. Each target was recorded for time 5000 s. Figure 2 shows a typical M X-ray spectrum for U.

3 Data analysis

The experimental M_i X-ray production cross-sections, σ^x_{Mi} ($\sigma^x_{M\alpha 1}, \sigma^x_{M\alpha 2}, \sigma^x_{M\beta}, \sigma^x_{M\zeta 1}, \sigma^x_{M\zeta 2}$) ($cm^2/g$) were evaluated by using the relation [12]

$$\sigma^x_M = \frac{N_{M^x}}{I_0 G \varepsilon_{M^x} \beta_{M^x} m}, \tag{1}$$

where $N_{M^x_i}$ ($N_{M_{\alpha 1}}, N_{M_{\alpha 2}}, N_{M_\beta}, N_{M_{\zeta 1}}, N_{M_{\zeta 2}}$) is the net counts per unit time under the associated elemental photopeak, $I_0 G$ is the intensity of exciting radiation falling on the sample, ε is the detector efficiency for the M X-rays of the element, m is the thickness of the target in g/cm^2 and β^x_M is the self-absorption given by [12]

$$\beta_{M^x} = \frac{1 - \exp\left[-\left(\frac{\mu_p}{\cos\theta_1} + \frac{\mu_e}{\cos\theta_2}\right)\right] m}{\left(\frac{\mu_p}{\cos\theta_1} + \frac{\mu_e}{\cos\theta_2}\right) m}, \tag{2}$$

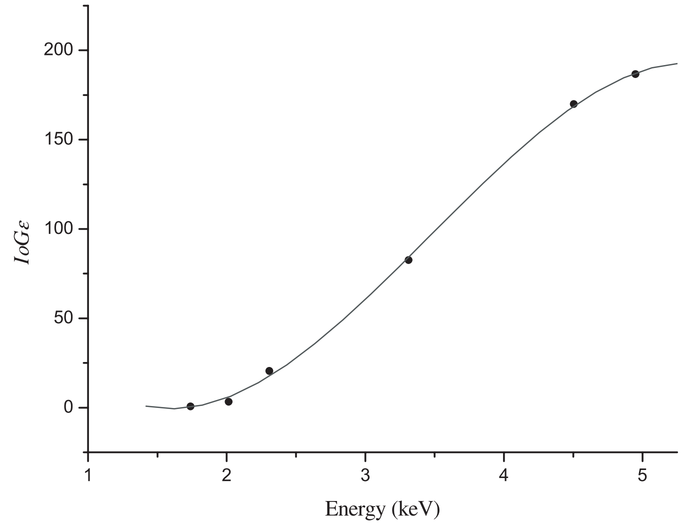

Fig. 3. Factor $I_0 G\varepsilon$ as a function of mean K X-ray energy.

where μ_p and μ_e are the total mass absorption coefficient of target at primary (5.96 keV) and emitter radiation energy [13] respectively, θ_1 and θ_2 are the angles of primary and emitted radiation with respect to the sample surface.

The term $I_0 G\varepsilon$, being the product of the incident photon flux, geometrical factor G and absolute efficiency ε of the X-ray detector, was determined by collecting the K X-ray spectra of samples of Si, P, S, KCO_3, TiO_2, and V_2O_3 in the same geometry using the equation:

$$I_0 G \varepsilon_K = \frac{N_K}{\beta_K m\, \sigma^x_K}, \tag{3}$$

where N_K, β_K and ε_K have the same meaning as in equation (1) except that they correspond to K X-rays instead of the M X-rays. The measured variation of $I_0 \mathrm{G}\varepsilon$ as a function of the mean K X-ray energy is as shown in Figure 3. σ^x_K represent the K X-ray fluorescence cross-sections and is given as

$$\sigma^x_K = \sigma^p_K \omega_K, \tag{4}$$

where σ^p_K is the K shell photoionization cross-section [14], ω_K is the K shell fluorescence yield [14].

By using the experimental M_i X-ray production cross-section values to obtained the $M_{4,5}$ X-ray production cross-sections were evaluated

$$\sigma^x_{M_{4,5}} = \sigma^x_{M_{\alpha 1}} + \sigma^x_{M_{\alpha 2}} + \sigma^x_{M_\beta} + \sigma^x_{M_{\zeta 1}} + \sigma^x_{M_{\zeta 2}} \tag{5}$$

$M_{4,5}$ subshells average fluorescence yields were evaluated using the relation:

$$\varpi_{M_{4,5}} = \frac{\sigma^x_{M_{4,5}}}{\sigma_4 + \sigma_5}, \tag{6}$$

where $\sigma_4(3d^{3/2})$ and $\sigma_5(3d^{5/2})$ are the M shell photoionization cross-section [14].

Experimental average M shell fluorescence (ϖ_M) yields were calculated as explained in our previous work [12].

Table 1. M subshell X-ray production cross-sections with theoretical values (cm^2/g).

Element	$\sigma^x_{M_{4,5}}$		$\sigma^x_{M_{\alpha\beta}}$	$\sigma^x_{M_\alpha}$	$\sigma^x_{M_\beta}$	$\sigma^x_{M_\zeta}$	
	Exp.	Theo.	Exp.	Theo.	Theo.	Exp.	Theo.
^{90}Th	19.125 ± 1.0	20.818	18.022 ± 1.1	11.213	7.840	1.103 ± 0.13	1.765
^{92}U	21.916 ± 1.3	23.031	20.525 ± 1.2	12.358	8.732	1.391 ± 0.15	1.941

Table 2. Average fluorescence yields with theoretical values.

Element	$\varpi_{M_{4,5}}$			ϖ_M		
	Present		Exp.	Theoretical predictions		
	Exp.	Theo.		Ref. [17]	Refs. [18,19]	Ref. [20]
^{90}Th	0.0656 ± 0.0058	0.0513	0.385± 0.0042	0.0543	0.0451	0.0453
^{92}U	0.0694 ± 0.0063	0.0568	0.0419±0.0050	-	0.0491	0.0502

4 Theoretical calculations

In this work we have calculated $M_{4,5}$ X-ray production cross-sections and $\varpi_{4,5}$ average fluorescence yields for the Th and U at 5.96 keV incident photon energy using the following equations:

$$\sigma^x_{M4} = [\sigma_{M1}(S_{14} + S_{12}S_{24} + S_{13}S_{34} + S_{12}S_{23}S_{34}) + \sigma_{M2}(S_{24} + S_{23}S_{34}) + \sigma_{M3}S_{34} + \sigma_{M4}]\omega_4 \quad (7)$$

$$\begin{aligned}\sigma^x_{M5} = [&\sigma_{M1}(S_{15} + S_{12}S_{25} + S_{13}S_3 + S_{14}S_{23}f_{45} \\ &+ S_{12}S_{23}S_{35} + S_{12}S_{24}f_{45} + S_{13}S_{34}f_{45} \\ &+ S_{12}S_{23}S_{34}f_{45}) + \sigma_{M2}(S_{25} + S_{24}f_{45} + S_{23}S_{35} \\ &+ S_{23}S_{34}f_{45} + \sigma_{M3}(S_{35} + S_{34}f_{45}) \\ &+ \sigma_{M4}f_{45} + \sigma_{M5}]\omega_5\end{aligned} \quad (8)$$

$$\sigma^x_{M_{4,5}} = \sum_{i=4-5} \sigma^x_{M_i} \quad (9)$$

where σ_{M_i} $(i = 4, 5)$ are the M shell photoionization cross-section [14], ω_i $(i = 4, 5)$ are the M sub-shell fluorescence yields, S_{ij} $(i = 1–3,\ j = 2–5)$ are Super Coster-Kronig transition probabilities and f_{45} Coster-Kronig transition probabilities [15].

Theoretical M X-ray productions cross-sections

$$\sigma^x_{M_\alpha} = \sigma^x_{M5}F_{5\alpha} \quad (10)$$

$$\sigma^x_{M_\zeta} = \sigma^x_{M4}F_{4\zeta 2} + \sigma^x_{M5}F_{5\zeta 1} \quad (11)$$

$$\sigma^x_{M_\beta} = \sigma^x_{M4}F_{4\beta} \quad (12)$$

where F_{ij} ($F_{5\alpha}$, $F_{5\zeta1}$, $F_{4\zeta2}$, and $F_{4\beta}$) are the fraction of the radiative transitions of the sub-shell M_i ($i = 4$ and 5) contained in the jth spectral line.

The F_{ij} values are given by the following

$$F_{5\alpha} = \frac{\Gamma(M_5 - N_6) + \Gamma(M_5 - N_7)}{\Gamma_5} \quad (13)$$

$$F_{5\zeta1} = \frac{\Gamma(M_5 - N_3)}{\Gamma_5} \quad (14)$$

$$F_{4\zeta1} = \frac{\Gamma(M_4 - N_2)}{\Gamma_4} \quad (15)$$

$$F_{4\beta} = \frac{\Gamma(M_4 - N_6)}{\Gamma_4} \quad (16)$$

where Γ_i ($i = 4$ and 5) is total radiative width of M_i sub-shell. This values obtained radiative transition probabilities to fill a vacancy in the M_4 and M_5 sub-shells [16].

Theoretical average $M_{4,5}$ subshells fluorescence yields were calculated for Th and U using the following relation

$$\varpi_{M_{4,5}} = 0.4\,(\omega_4 + f_{45}\omega_5) + 0.6\omega_5. \quad (17)$$

This relation has been based on the consideration that the contribution of M_4 and M_5 sub-shells to total M X-ray production cross-sections is about 80% [3].

5 Results and discussion

Experimental $\sigma^x_{M_{4,5}}$, X-ray production cross-sections for Th and U, measured for incident photon energies 5.96 keV, are presented in Table 1 and compared with theoretical values. Similarly, $\omega_{M_{4,5}}$ average fluorescence yield values are listed in Table 2 and compared with theoretical values.

The overall error in present measurements is estimated to be 7–10%. This error is due to the evaluation of peak areas (≤3%), the product $I_0G\varepsilon$ (5–7%), sample thickness measurements (≈4%), and the absorption correction factor (≤2%).

We have derived the absolute cross-sections for $M_{\alpha\beta}$ and M_ζ X-rays line as well as the total M production X-ray cross-sections. We have found M_ζ X-ray production cross-section values effected on total M shell X-ray cross-section weak (about 8% of total M shell X-ray cross-section). $M_{\alpha\beta}$ X-rays line arises due to vacancy in the M_4 and M_5 sub-shells. The contribution of M_4 and M_5 sub-shells to total M X-ray production cross-sections is about 92%.

The experimental average M shell fluorescence yields are in good agreement with the theoretical estimates based on relativistic Dirac–Hartree–Slater theory. $M_{4,5}$ subshells average fluorescence yields ($\varpi_{M_{4,5}}$) values 22–27% higher than calculated theoretical values. The results for average fluorescence yields (ϖ_M) are 14.6% and 15–16.5% larger than the theoretical values of Chen [18,19] and Hubbell [20], respectively. The discrepancy between the measured and theoretical values of average fluorescence yield may be due to systematic errors in the physical parameters.

References

1. R. Gowda, D. Powers, Phys. Rev. A **31**, 134 (1985)
2. M. Pajek, A.B. Kobzev, S. Sandrik, A.V. Skrpnik, R.A. Ilkhamov, S.H. Khusmurodov, G. Lapicki, Phys. Rev. A **41**, 261 (1990)
3. J.S. Braich, P. Verma, H.R. Verma, J. Phys. B: At. Mol. Opt. Phys. **30**, 2359 (1997)
4. A. Amirabadi, H. Afarideh, S.M. Haji-Saeid, F. Shokouhi, H. Peyrovan, J. Phys. B: At. Mol. Opt. Phys. **30**, 863 (1997)
5. Y. Singh, L.C. Tribedi, Phys. Rev. A **66**, 062709 (2002)
6. Y. Singh, L.C. Tribedi, Nucl. Instrum. Meth. B **205**, 794 (2003)
7. K. Shatendra, K.L. Allawadhi, B.S. Sood, Physica C **124**, 279 (1984)
8. R.R. Garg, S. Singh, J.S. Shahi, D. Metha, N. Singh, P.N. Trehan, S. Kumar, M.L. Garg, P.C. Mangal, X-ray Spectrom. **20**, 91 (1991)
9. R.C. Jopson, H. Mark, C.D. Swift, M.A. Williamson, Phys. Rev. A **5**, 1353 (1965)
10. M. Deutsch, O. Gang, G. Hölzer, J. Härtwig, J. Wolf, M. Fritsch, E. Förster, Phys. Rev. A **52**, 3661 (1995)
11. D.V. Rao, R. Cesareo, G.E. Gigante, Radiat. Phys. Chem. **49**, 503 (1997)
12. G. Apaydın, E. Tıraşoğlu, U. Çevik, B. Ertuğral, H. Baltaş, M. Ertuğrul, A.İ. Kobya, Radiat. Phys. Chem. **72**, 549 (2005)
13. E. Storm, I. Israel, Nucl. Data Tables A **7**, 565 (1970)
14. J.H. Scofield, UCRL Report 51326 (1973) Lawrence Livermore Laboratory, Livermore, CA
15. Ö. Söğüt, E. Büyükkasap, A. Küçükönder, M. Ertuğrul, O. Doğan, H. Erdoğan, Ö. Şimşek, X-ray Spectrom. **31**, 62 (2002)
16. C.P. Bhalla, J. Phys. B: At. Mol. Opt. Phys. **3**, 916 (1970)
17. E.J. McGuire, Phys. Rev. A **5**, 1043 (1975)
18. M.H. Chen, B. Crasemann, H. Mark, Phys. Rev. A **21**, 449 (1980)
19. M.H. Chen, B. Crasemann, H. Mark, Phys. Rev. A **27**, 2989 (1983)
20. J.H. Hubbell, NISTIR Report 89 (1989) p. 4144